J. Cell. Mol. Med. Vol 14, No 8, 2010 pp. 2109-2121

Fibroblast growth factor 2-antagonist activity of a long-pentraxin 3-derived anti-angiogenic pentapeptide

Daria Leali [a], Roberta Bianchi [a], Antonella Bugatti [a], Stefania Nicoli [a], Stefania Mitola [a], Laura Ragona [b], Simona Tomaselli [b], Grazia Gallo [c], Sergio Catello [d], Vincenzo Rivieccio [d], Lucia Zetta [b], Marco Presta [a, *]

[a] Unit of General Pathology and Immunology, Department of Biomedical Sciences and Biotechnology, School of Medicine, University of Brescia, Brescia, Italy
[b] Istituto per lo Studio delle Macromolecole, Consiglio Nazionale delle Ricerche, Milan, Italy
[c] Sigma-Tau R&D, Pomezia, Rome, Italy
[d] Tecnogen S.p.A, Piana di Monteverna, Caserta, Italy

Received: February 3, 2009; Accepted: April 28, 2009

Abstract

Fibroblast growth factor-2 (FGF2) plays a major role in angiogenesis. The pattern recognition receptor long-pentraxin 3 (PTX3) inhibits the angiogenic activity of FGF2. To identify novel FGF2-antagonistic peptide(s), four acetylated (Ac) synthetic peptides overlapping the FGF2-binding region PTX3-(97–110) were assessed for their FGF2-binding capacity. Among them, the shortest pentapeptide Ac-ARPCA-NH_2 (PTX3-[100–104]) inhibits the interaction of FGF2 with PTX3 immobilized to a BIAcore sensorchip and suppresses FGF2-dependent proliferation in endothelial cells, without affecting the activity of unrelated mitogens. Also, Ac-ARPCA-NH_2 inhibits angiogenesis triggered by FGF2 or by tumorigenic FGF2-overexpressing murine endothelial cells in chick and zebrafish embryos, respectively. Accordingly, the peptide hampers the binding of FGF2 to Chinese Hamster ovary cells overexpressing the tyrosine-kinase FGF receptor-1 (FGFR1) and to recombinant FGFR1 immobilized to a BIAcore sensorchip without affecting heparin interaction. In all the assays the mutated Ac-ARP *S*A-NH_2 peptide was ineffective. In keeping with the observation that hydrophobic interactions dominate the interface between FGF2 and the FGF-binding domain of the Ig-like loop D2 of FGFR1, amino acid substitutions in Ac-ARPCA-NH_2 and saturation transfer difference-nuclear magnetic resonance analysis of its mode of interaction with FGF2 implicate the hydrophobic methyl groups of the pentapeptide in FGF2 binding. These results will provide the basis for the design of novel PTX3-derived anti-angiogenic FGF2 antagonists.

Keywords: angiogenesis • FGF • pentraxin • BIAcore • NMR • receptors • heparan sulphate • zebrafish • chorioallantoic membrane • embryo • tumour

Introduction

Angiogenesis is the process of generating new capillary blood vessels. In the adult, angiogenesis occurs under tight regulation in the female reproductive system and during wound healing. Uncontrolled neovascularization is observed in tumour growth and in angioproliferative diseases [1]. Tumours cannot grow larger than a few square millimetres as a mass unless a new blood supply is induced [2]. Hence the control of the neovascularization process may affect tumour growth and represents a novel approach to angiogenesis-dependent disease therapy, including neoplasia [3].

Fibroblast growth factor-2 (FGF2) is a major heparin-binding angiogenic growth factor that induces cell proliferation, chemotaxis and protease production in cultured endothelial cells [4]. *In vivo*, FGF2 shows angiogenic activity in different experimental models [5] and modulates neovascularization during wound healing, inflammation, atherosclerosis and tumour growth [6], thus representing a possible target for anti-angiogenic therapies [7, 8]. Accordingly, preclinical studies demonstrate that FGF2 antagonists inhibit tumour growth and vascularization [8–10].

FGF2 exerts its activity on endothelial cells by interacting with high affinity tyrosine-kinase FGF receptors (FGFRs) [11] and low affinity heparan sulphate proteoglycans (HSPGs) [12, 13], leading

*Correspondence to: Marco PRESTA,
General Pathology, Dept. Biomedical Sciences and Biotechnology,
Viale Europa 11, 25123 Brescia, Italy.
Tel.: +39-30-3717311
Fax: +39-30-3701157
E-mail: presta@med.unibs.it

doi:10.1111/j.1582-4934.2009.00855.x

to the formation of productive HSPG/FGF2/FGFR ternary complexes [14]. Therefore, natural and synthetic molecules able to interfere with HSPG/FGF2/FGFR interaction may act as angiogenesis inhibitors (reviewed in [8]). To this respect, structural analysis of FGFR ligands and screening of random phage epitope libraries have led to the design of synthetic peptides able to target FGFRs and compete for ligand binding, thus inhibiting the biological activity of FGF2 [15–22]. Similarly, FGF2-binding peptides have been identified as *in vitro* and/or *in vivo* FGF2 antagonists [23–25].

The pattern recognition receptor pentraxin 3 (PTX3) is the prototypic member of the long PTX family. It shares the C-terminal PTX domain with short PTXs and possesses a unique N-terminal domain. The biological activity of PTX3 is related to its ability to interact with different ligands *via* its N-terminal or C-terminal domain as a consequence of the modular structure of the protein [26, 27]. Recent observations have shown that PTX3 binds FGF2 with high affinity and specificity [28]. Accordingly, PTX3 inhibits FGF2-dependent endothelial cell proliferation *in vitro* and angiogenesis *in vivo* [28]. Also, PTX3 inhibits FGF2-dependent smooth muscle cell activation and intimal thickening after arterial injury [29]. An integrated approach that utilized PTX3-related synthetic peptides, monoclonal antibodies and surface plasmon resonance analysis has identified a FGF2-binding domain in the N-terminal extension of PTX3 spanning the PTX3-(97–110) region, thus suggesting that synthetic peptides related to the PTX3-(97–110) sequence may represent novel PTX3-derived FGF2 antagonists [30].

Here, we have investigated the ability of various PTX3-(97–110)-related synthetic peptides to interact with FGF2. The results identify the short acetylated (Ac) pentapeptide Ac-ARPCA-NH_2 (in single letter code), corresponding to PTX3-(100–104) sequence, as the minimal FGF2-binding peptide able to interfere with FGF2/FGFR interaction. Accordingly, the peptide is endowed with a significant FGF2-antagonist activity *in vitro* and *in vivo*. Nuclear magnetic resonance (NMR) analysis of the interaction mode of Ac-ARPCA-NH_2 with FGF2 points to a pivotal role of the N-terminal blocking methyl group and of the methyl group of the side chain of Ala5 residue in FGF2 interaction. These results will provide the basis for the design of novel PTX3-derived FGF2 antagonists.

Methods

Chemicals

Human recombinant FGF2, human recombinant PTX3 and synthetic PTX3-derived peptides (HPLC purity $\geq$95%) were provided by Tecnogen (Piana di Monteverna, Caserta, Italy). FGF2 and PTX3 were expressed in *Escherichia coli* and Chinese hamster ovary (CHO) cells, respectively, and purified as described [31, 32]. Amino acid numbering starts from the methionine residue in position 1 in the human PTX3 leader sequence. Recombinant FGF8b was provided by M. Jalkanen (Biotie, Turku, Finland). 1,2-dioctanoyl-sn-glycerol (DAG), epidermal growth factor (EGF), 12-O-tetradecanoyl phorbol 13-acetate (TPA) and vascular endothelial growth factor-165 isoform (VEGF) were from Calbiochem (La Jolla, CA, USA). FGF1 was from Peprotech (London, United Kingdom). Recombinant human sFGFR1(IIIc)/Fc and sKDR/Fc chimeras were from RELIATech GmbH (Braunschweig, Germany).

Cell cultures

Foetal bovine aortic GM7373 endothelial cells [28] were grown in Dulbecco's modified Eagle's medium (DMEM) containing 10% foetal calf serum (FCS). Wild-type CHO-K1 cells and the derived HSPG-deficient A745 CHO cell mutants [33], kindly provided by J.D. Esko (La Jolla, CA, USA), were grown in Ham's F-12 medium supplemented with 10% FCS. FGFR1-transfected A745 CHO flg-1A cells, bearing about 30,000 FGFR1 molecules/cell, were generated in our laboratory by transfection with the IIIc variant of murine FGFR1 cDNA [34]. CHO cells stably overexpressing murine FGFR1, FGFR2 or FGFR3, or human FGFR4 (10,000 to 100,000 receptors per cell) were generated in our laboratory by transfection with the IIIc variant of the corresponding receptor cDNA [35]. Tumorigenic, FGF2-overexpressing murine aortic endothelial FGF2-T-MAE cells [36] were grown in DMEM *plus* 10% FCS.

Cell proliferation assays

GM7373 cell proliferation assay was performed as described [37]. Briefly, subconfluent cultures of GM7373 cells were incubated in medium containing 0.4% FCS *plus* FGF2 (0.55 nM) in the absence or the presence of different antagonists. In a second set of experiments, GM7373 cells were incubated in medium containing 0.4% FCS *plus* the indicated mitogenic stimuli in the absence or the presence of Ac-ARPCA-NH_2 peptide (66 μM). Furthermore, FGFR1-, FGFR2-, FGFR3- and FGFR4-transfected CHO cells were seeded in 96-well plates at 30,000 cells/cm^2. After 16 hrs, cells were incubated in medium containing 0.4% FCS *plus* FGF2 (0.55 nM) in the absence or the presence of Ac-ARPCA-NH_2 or Ac-ARP*S*A-NH_2 peptides (both at 300 μM). For all the assays, cells were trypsinized and counted in a Burker chamber after 24 hrs of incubation.

FGF2-mediated cell–cell adhesion assay

This assay was performed as described previously [38], with minor modifications. Briefly, wild-type CHO-K1 cells were seeded in 24-well plates at 150,000 cells/cm^2. After 24 hrs, cell monolayers were washed with PBS and incubated with 3% glutaraldehyde in PBS for 2 hrs at 4°C. Fixation was stopped with 0.1 M glycine, and cells were washed extensively with PBS. Then, A745 CHO flg-1A cells (50,000 cells/cm^2) were added to CHO-K1 monolayers in serum-free medium *plus* 10 mM EDTA with or without 1.66 nM FGF2 in the absence or presence of increasing concentrations of the competitor under test. After 2 hrs of incubation at 37°C, unattached cells were removed by washing twice with PBS, and A745 CHO flg-1A cells bound to the CHO-K1 monolayer were counted under an inverted microscope at $\times$125 magnification. Adherent A745 CHO flg-1A cells have a rounded morphology and can be easily distinguished from the confluent CHO-K1 monolayer lying underneath on a different plane of focus. Data are expressed as the mean of the cell counts of three microscopic fields chosen at random. All experiments were performed in triplicate and repeated twice with similar results.

Western blot analysis

Mitogen-activated protein kinase ($ERK_{1/2}$) phosphorylation assay was performed as described [34] with minor modifications. Briefly, GM7373 cells were grown to 80–90% confluence in 48-well plates and starved for 2 hrs in medium containing 0.4% FCS. After pre-incubation for 30 min. at 37°C with or without synthetic peptides (1.0 mM final concentration), cells were treated with FGF2 (0.17 nM) for 10 min. without changing the medium. At the end of the incubation, cells were washed briefly with ice-cold PBS, lysed in reducing SDS-PAGE sample buffer, sonicated at 50 W for 20 sec., and boiled. Samples were analysed by Western blotting using a monoclonal anti-phospho-$ERK_{1/2}$ antibody and a monoclonal anti-ERK_2 antibody (both at 1/1000 dilution, Santa Cruz Biotechnology, Inc., Santa Cruz, CA, USA), followed by incubation with peroxidase-conjugated goat antimouse IgG antibody (1/5000 dilution, Sigma, St. Louis, MO, USA).

BIAcore binding assay

A BIAcore X apparatus (BIAcore Inc., Piscataway, NJ, USA) was used to set up four different experimental models. (*i*) PTX3-derived peptides were analysed for their capacity to inhibit the binding of free FGF2 to PTX3 immobilized to the sensor chip. To this purpose, PTX3 (2.2 μM in 10 mM sodium acetate, pH 2.4) was allowed to react with a flow cell of a CM4 sensor chip that was previously activated with a mixture of 0.2 M N-ethyl-N′-(3-dimethylaminopropyl)-carbodiimide hydrochloride and 0.05 M N-hydroxysuccinimide (35 μl, flow rate 10 μl/min.). These experimental conditions allowed the immobilization of ~0.1 pmol/mm^2 of PTX3. Similar results were obtained for immobilization of gelatin, here used as a negative control and for blank subtraction. After ligand immobilization, matrix neutralization was performed with 1.0 M ethanolamine (pH 8.5) (35 μl, flow rate 10 μl/min.). (*ii*) PTX3-derived peptides were analysed for their capacity to inhibit the binding of free FGF2 to immobilized heparin, prepared as described previously [39]. Briefly, size-defined heparin (13.6 kD) was biotinylated on its reducing end, and a flow cell of a CM3 sensor chip was activated with streptavidin. Then, biotinylated heparin was allowed to react with the streptavidin-coated sensor chip. (*iii*) PTX3-derived peptides were analysed for their capacity to inhibit the binding of free FGF2 to immobilized FGFR1. To this purpose, protein A (100 μg/ml in 10 mM sodium acetate, pH 4.8) was allowed to react with a flow cell of a CM5 sensor chip that was previously activated with a mixture of 0.2 M N-ethyl-N′-(3-dimethylaminopropyl)-carbodiimide hydrochloride and 0.05 M N-hydroxysuccinimide (35 μl, flow rate 10 μl/min.). Following neutralization with 1.0 M ethanolamine (pH 8.5) (35 μl, flow rate 10 μl/min.), recombinant human sFGFR1(IIIc)/Fc chimera (100 μg/ml) was allowed to react with the protein A-coated sensor chip. Then, a 30-sec. injection of a mixture (7 μl, flow rate 15 μl/min.) of 0.2 M N-ethyl-N′-(3-dimethylaminopropyl)-carbodiimide hydrochloride and 0.05 M N-hydroxysuccinimide was performed, followed immediately by a 30-sec. injection of 1.0 M ethanolamine (pH 8.5) (7 μl, flow rate 15 μl/min.). These experimental conditions allowed the immobilization of ~0.003 pmol/mm^2 of sFGFR1(IIIc)/Fc chimera. Protein A-coated sensorchip was used as a negative control and for blank subtraction. (*iv*) PTX3-derived peptides were analysed for their capacity to inhibit the binding of free VEGF to immobilized VEGFR2/KDR. To this purpose, sKDR/Fc chimera (20 μg/ml in 10 mM sodium acetate, pH 5.3) was allowed to react with a flow cell of a CM5 sensor chip that was previously activated with a mixture of 0.2 M N-ethyl-N′-(3-dimethylaminopropyl)-carbodiimide hydrochloride and 0.05 M N-hydroxysuccinimide (35 μl, flow rate 10 μl/min.). These experimental conditions allowed the immobilization of ~0.06 pmol/mm^2 of sKDR/Fc chimera. After ligand immobilization, matrix neutralization was performed with 1.0 M ethanolamine (pH 8.5) (35 μl, flow rate 10 μl/min.). Depending upon the experimental model, different doses of FGF2 were injected in the presence of increasing concentrations of the peptide under test in 0.01 M Hepes pH 7.4 *plus* 0.005% surfactant P20, 0.15 M NaCl, 3 mM ethylenediaminetetraacetic acid (HBS-EP buffer). Injection lasted for 4 min. to allow the association of FGF2 with the immobilized ligand. In parallel experiments, 45 nM VEGF was injected for 4 min. on the sKDR/Fc surface in the absence or presence of 300 μM Ac-ARPCA-NH_2 peptide. The response (in RU) was recorded at the end of injection, and binding data were plotted as percentage of maximal bound analyte.

Chick embryo chorioallantoic membrane assay

Alginate beads (5 μl) containing vehicle or 8 pmoles of FGF2 with or without synthetic peptides (117 nmoles) were prepared as described [40] and placed on top of the chicken embryo chorioallantoic membrane (CAM) of fertilized White Leghorn chicken eggs at day 11 of incubation (10 eggs per experimental group). After 72 hrs, blood vessels converging towards the implant were counted by two observers in a double-blind fashion under a stereomicroscope (STEMI-SR, ×2/0.12; Zeiss, Arese, Italy).

Zebrafish/tumour xenograft angiogenesis assay

This was performed as described previously [41, 42]. Briefly, a zebrafish (*Danio rerio*) breeding colony (wild-type AB strain) was maintained at 28°C at the Zebrafish Facility of the University of Brescia. Dechorionated embryos at 48 hrs after fertilization were anaesthetized with 0.04 mg/ml of tricaine (Sigma) and injected with 1000 to 2000 FGF2-T-MAE cells per embryo resuspended in 3–4 nl of Matrigel (Becton Dickinson, Milan, Italy) in the absence or in the presence of Ac-ARPCA-NH_2 or Ac-ARP*S*A-NH_2 peptides (each at 75 μM) using a Picospritzer microinjector (Eppendorf, Hamburg, Germany). After 24 hrs, zebrafish embryos were fixed in 4% paraformaldehyde for 2 hrs at room temperature and stained for endogenous alkaline phosphatase activity [43]. Then, embryos were mounted in agarose-coated Petri dishes, photographed under an epifluorescence Leica MZ16 F stereomicroscope equipped with a DFC480 digital camera (Leica, Solms, Germany), and scored for a positive angiogenic response defined as the presence of a new alkaline phosphatise-positive microvasculature projecting from the sub-intestinal vessel plexus of the embryo and infiltrating the tumour graft [41, 42].

Nuclear magnetic resonance spectroscopy

Ac-ARPCA-NH_2, Ac-*G*RPCA-NH_2, Ac-ARPC*G*-NH_2, Ac-ARP*S*A-NH_2 and the non-acetylated *H*-ARPCA-NH_2 peptides were dissolved at 1.6 mM final peptide concentration in 30 mM phosphate buffer, 40 mM NaCl, pH 6.8. 1,4-Dithiothreitol (DTT) was added to peptide solutions at a final concentration of 8 mM in order to avoid the production of dimers through the formation of disulphide bridges between the free cysteines. In order to investigate the interaction between peptides and FGF2, samples of 50 μM protein were prepared in the presence of 1.9 mM peptide in 30 mM phosphate buffer (95% D_2O, 5% H_2O), 8.0 mM DTT, 40 mM NaCl, pH 6.8.

All NMR spectra were recorded on DMX spectrometer (Bruker, Ettlingen, Germany) operating at 500 MHz equipped with a triple resonance

probehead, incorporating gradients in the *z*-axis. All data were collected at 280 K on a spectral width of 6510 Hz. TOCSY, ROESY and NOESY spectra were recorded using standard sequences [44, 45]. A spin lock time of 80 msec. was used for TOCSY, mixing times of 150 and 250 msec. were used for ROESY spectra, while different NOESY spectra were collected with mixing times of 100, 180, 250 and 400 msec. on peptide alone and in the presence of FGF2 at 1:40 ratio at 280 and 290 K. Longitudinal relaxation times T_1 of the peptides were measured when the FGF2 protein was present. The standard inversion recovery method was used for the measurements with a relaxation delay of 8 sec. Data points (16 K) were acquired to cover a sweep width of 10 ppm. Data were analysed using Bruker Topspin software. T_1 values were found to be rather constant along the peptide side chains in a range of 0.4–0.6 sec., except for longer T_1 observed for methyl protons of N-terminal acetyl group (1.1 sec.).

For the acquisition of saturation transfer difference (STD) NMR [45, 46], a 1D pulse sequence incorporating a $T_{1\rho}$ filter to remove disturbing protein signals was used. Spectra were recorded with a spectral width of 6510 Hz and 32 K data points. On-resonance irradiations were performed at different frequencies in the aromatic (3325 Hz) and methyl (−216 Hz, −150 Hz) regions and off-resonance irradiation was performed at –20,000 Hz, using a series of Gaussian pulses with a 1% truncation and 50 msec. duration to give total saturation times of 0.25, 0.5, 1, 2, 2.5, 3, 4, 4.5 sec. Given the low molecular weight of FGF2 (18 kD), a compromise was found between the high power saturation pulses needed for full protein saturation by spin-diffusion and the low power saturation pulses needed to avoid direct irradiation of peptide resonances. The selective saturation of the protein was checked by collecting a STD control spectrum in the same experimental conditions on the ligand alone which did not show any signal, thus excluding direct excitation of the peptide resonances. The duration of the $T_{1\rho}$ filter was 30 msec. STD NMR spectra were acquired with a total of 192 transients in addition to 32 scans to allow the sample to come to equilibrium. STD spectrum was obtained by subtraction of saturated spectrum from the reference spectrum obtained with off resonance irradiation. STD intensities of individual signals (I_{STD}) were measured relative to the corresponding signal intensity in the reference spectrum (I_0) and described by STD factor $A_{STD} = (I_{STD})/I_0$. Titration of FGF2 protein with Ac-ARPCA-NH_2 was performed by adding different amounts of a stock solution of the peptide to a 50 μM FGF2 sample. STD experiments were acquired on samples ranging between 1:10 and 1:100 FGF2:Ac-ARPCA-NH_2 molar ratios at 280 K on a 500 MHz spectrometer using 3 sec. saturation time.

Computational methods

A conformational analysis was performed on Ac-ARPCA-NH_2 peptide based on low mode Montecarlo procedure with OPLS-AA force field using water as implicit solvent (software: Macromodel v.9.5 Schrodinger llc). 3000 conformers within 10 kcal/mol were analysed and divided into three clusters. The most stable conformational family (ΔE within 3 kcal/mol) showed a type-I β-turn between Pro and Cys residues and the nearest distance between Ala1 and Ala5 (mean value = 6.6 ± 1.5 Å), whereas the other two families showed a progressive tendency to form a random coil conformation. The global minimum conformation of Ac-ARPCA-NH_2 was permitted to rotate at N- and C-terminal portion and superimposed to the crystal structure of FGFR1 (PDB code: 1FQ9) in the β-sheet portion 164–170 of the hydrophobic domain D2 of the receptor. The complex was then minimized and the peptide maintained its characteristic β-turn after minimization.

Results

Identification of PTX3-(100–104) as a minimal linear FGF2 binding sequence

Previous observations had shown that a 14 mer PTX3-(97–110) peptide binds to FGF2, thus preventing FGF2/PTX3 interaction and inhibiting FGF2-dependent endothelial cell proliferation *in vitro* and angiogenesis *in vivo* [30]. On this basis, in an attempt to identify novel FGF2-antagonist(s), four acetylated (Ac) overlapping synthetic peptides based on the amino acid sequences PTX3-(97–107), PTX3-(100–113), PTX3-(100–104) and PTX3-(104–113) were compared with PTX3-(97–110) peptide for their capacity to interact with FGF2 (Table 1). In a first set of experiments, surface plasmon resonance was exploited to assess the ability of increasing concentrations of these peptides (ranging from 3 to 3000 μM) to compete for the binding of free FGF2 to PTX3 immobilized onto a BIAcore sensor chip [30] (Table 1). Among the peptides tested, PTX3-(100–104) was the most active in preventing FGF2/PTX3 interaction (ID_{50} = 120 μM), PTX3-(97–107) and PTX3-(100–113) showed an activity similar to the parental peptide PTX3-(97–110) (ID_{50} = 300–500 μM), whereas PTX3-(104–113) was almost inactive (ID_{50} = 2.0 mM). In keeping with their ability to bind FGF2 in the mobile phase, PTX3-(97–110), PTX3-(100–113), PTX3-(97–107) and PTX3-(100–104) all inhibited the mitogenic activity exerted by FGF2 on endothelial GM7373 cells in a dose-dependent manner (ID_{50} values ranging between 15 and 50 μM), whereas PTX3-(104–113) was ineffective (Table 1). Taken together, the data suggest that the amino acid sequence ARPCA (in single letter code), which is present in all the active peptides and absent in the inactive PTX3-(104–113) peptide (Table 1), may represent a minimal linear FGF2-binding amino acid sequence in the PTX3-(97–110) region endowed with FGF2 antagonist activity.

To assess the relevance of each amino acid residue of Ac-ARPCA-NH_2 pentapeptide for FGF2 interaction, a series of synthetic peptides carrying different amino acid substitutions were tested for their FGF2 antagonist activity as evaluated by the capacity to prevent FGF2/PTX3 interaction by surface plasmon resonance analysis and to inhibit FGF2-dependent endothelial cell proliferation. As shown in Table 2, the partially scrambled Ac-A*PCR*A-NH_2 and the scrambled Ac-*PARAC*-NH_2 peptides showed an inhibitory activity that was significantly reduced or abolished in both assays, pointing to the relevance of the relative position of each residue for the FGF2 antagonist capacity of the peptide. Also, the FGF2 antagonist activity was dramatically reduced for the non-acetylated *H*-ARPCA-NH_2 peptide and for the Ac-ARPC*G*-NH_2 and Ac-*G*RPC*G*-NH_2 peptides, but not for the Ac-*G*RPCA-NH_2 peptide, indicating a role for the N-terminal blocking methyl group and for the methyl group of the side chain of Ala5 residue in FGF2 interaction. The activity was lost also when the Arg2 residue was replaced in Ac-A*L*PCA-NH_2 peptide, when the Pro3 residue was replaced in Ac-AR*A*CA-NH_2 and Ac-AR*G*CA-NH_2 peptides, or when the Cys4 residue was replaced in Ac-ARP*S*A-NH_2, Ac-ARP*V*A-NH_2 and Ac-ARP*M*A-NH_2 peptides, thus underlying the role of the RPC

Table 1 FGF2-antagonist activity of PTX3-derived synthetic peptides

PTX3 peptide	Amino acid sequence*	FGF2/PTX3 interaction in BIAcore ID50 (μM)	FGF2-dependent EC proliferation ID50 (μM)
PTX3-(97–110)	Ac-ESLARPCAPGAPAE-NH_2	300	20
PTX3-(97–107)	Ac-ESLARPCAPGA-NH_2	300	50
PTX3-(100–113)	Ac-ARPCAPGAPAEARL-NH_2	500	10
PTX3-(100–104)	Ac-ARPCA-NH_2	120	15
PTX3-(104–113)	Ac-APGAPAEARL-NH_2	2000	>1000

Peptides were tested for their capacity to inhibit the interaction of free FGF2 (150 nM) with PTX3 immobilized onto a BIAcore sensorchip and to inhibit the mitogenic activity exerted by FGF2 on endothelial GM7373 cells. The experiments were performed with concentrations of peptide ranging between 3 and 3000 μM and between 3 and 1000 μM for the two assays, respectively, and ID_{50} values were calculated from the plotted dose–response curves. Data are representatives of two to three independent experiments in triplicate.

*Amino acid sequences are shown in the single letter code and numbering starts from the methionine residue in position 1 in the PTX3 leader sequence.

amino acid sequence in Ac-ARPCA-NH_2/FGF2 interaction. Interestingly, the FGF2 antagonist activity was lost also when the ARPCA region was mutated within synthetic peptides based on the amino acid sequence PTX3-(97–110), as observed for peptides Ac-ESL*G*RPC*G*PGAPAE-NH_2, Ac-ESLAR*G*CAPGAPAE-NH_2 and Ac-ESLARP*S*APGAPAE-NH_2 when compared to the wild-type Ac-ESLARPCAPGAPAE-NH_2 peptide (data not shown). Similar results were obtained when the same amino acid substitutions were performed in the longer FGF2-antagonist PTX3-(82–110) peptide [30], thus confirming the importance of the linear ARPCA sequence in FGF2 interaction (data not shown).

Taken together, the results identify the Ac-ARPCA-NH_2 pentapeptide as a synthetic FGF2 antagonist. N-terminal blocking and Ala5 side-chain methyl groups, as well as RPC residues, all appear to play a non-redundant role in FGF2 interaction. On this basis, the Ac-ARPCA-NH_2 pentapeptide (hereafter referred to as ARPCA) was characterized further for its capacity to interact with FGF2 and to antagonize its biological activity.

ARPCA peptide inhibits FGF2/FGFR1 interaction

PTX3 is able to inhibit the mitogenic activity exerted by FGF2 and by other members of the FGF family on endothelial cells, without affecting the activity of unrelated mitogens [28]. On this basis, ARPCA was assessed for its capacity to affect the proliferation of endothelial GM7373 cells exposed to different mitogenic stimuli. In these and following biological experiments, the inactive Ac-ARP*S*A-NH_2 (hereafter referred to as ARPSA) was used as a negative control peptide. As shown in Fig. 1(A), ARPCA inhibits GM7373 cell proliferation triggered by FGF2, FGF8b and with a less efficiency by FGF1, whereas it does not affect the mitogenic activity of VEGF, EGF, DAG, TPA and serum. No inhibition was instead exerted by control peptide ARPSA on any mitogen. Moreover, in keeping with the capacity of FGF2 to interact with all four members of the FGFR family [47], ARPCA, but not ARPSA, inhibits the proliferation triggered by FGF2 in CHO cells stably transfected with the FGFR1, FGFR2, FGFR3 or FGFR4 isoforms [35] (Fig. 1B). These data demonstrate that, as for PTX3, the inhibitory activity of ARPCA is limited to the FGF/FGFR system and it is not due to a generic antiproliferative/toxic effect.

FGFs exert their biological activity by leading to the formation of a productive HSPG/FGF/FGFR ternary complex [14]. On this basis, to investigate the molecular mechanism responsible of its FGF2 antagonist activity, ARPCA was evaluated for the capacity to prevent the formation of HSPG/FGF2/FGFR1 ternary complexes in a cell–cell adhesion model in which FGF2 mediates the interaction of HSPG-deficient CHO cells stably transfected with FGFR1 to a monolayer of CHO-K1 cells expressing HSPGs but not FGFRs [38]. As shown in Fig. 2(A), ARPCA, but not ARPSA, exerts a significant inhibitory activity on FGF2-mediated cell–cell adhesion (ID_{50} equal to 50 μM and >1.0 mM for the two peptides, respectively), thus indicating the capacity of the peptide to interfere with HSPG/FGF2/FGFR1 complex formation. Accordingly, ARPCA, but not ARPSA, inhibits FGF2-induced $ERK_{1/2}$ phosphorylation in GM7373 cells [34], thus demonstrating the capacity of the peptide to affect FGFR signalling (Fig. 2B).

To assess whether the inhibition of HSPG/FGF2/FGFR1 complex formation by ARPCA is due to its ability to hamper HSPG/FGF2 and/or FGF2/FGFR1 interactions, the peptide was investigated for the capacity to prevent the binding of free FGF2 to heparin or to a sFGFR1(IIIc)/Fc chimera both immobilized to BIAcore sensor chips. As shown in Fig. 2(C), ARPCA does not affect FGF2/heparin interaction ($ID_{50} > 1.0$ mM) whereas it significantly inhibits the binding of FGF2 to the immobilized receptor with a potency ($ID_{50} = 30$ μM) similar to that found when the peptide was tested for its capacity to inhibit FGF2-mediated endothelial cell proliferation ($ID_{50} = 15$ μM, see Table 1). No effect was instead exerted by ARPSA on both sensor chips. In a control experiment, ARPCA did not prevent the binding of VEGF to an immobilized sKDR/Fc chimera (data not shown), in keeping with the incapacity of the peptide to affect the mitogenic activity exerted by VEGF on endothelial cells (see Fig. 1A).

Taken together these data indicate that the FGF2 antagonist activity of ARPCA is related to its ability to interfere with

Table 2 FGF2-antagonist activity of Ac-ARPCA-NH_2 peptide mutants

		Assay	
Amino acid substitution(s)	**Synthetic peptide (amino acid sequence)**	**FGF2/PTX3 interaction in BIAcore ID_{50} (μM)**	**FGF2-dependent EC proliferation ID_{50} (μM)**
None			
	Ac-ARPCA-NH_2	120	15
Amino acid position			
	Ac-A*PCR*A-NH_2	800	100
	Ac-*PARAC*-NH_2	1000	>1000
N-terminus blockade			
	H-ARPCA-NH_2	2000	500
Ala residues			
	Ac-*G*RPCA-NH_2	80	15
	Ac-ARPC*G* -NH_2	1000	>1000
	Ac-*G*RPC*G*-NH_2	>3000	1000
Arg residue			
	Ac-A*L*PCA-NH_2	>3000	>1000
Pro residue			
	Ac-AR*A*CA-NH_2	>3000	>1000
	Ac-AR*G*CA-NH_2	1500	500
Cys residue			
	Ac-ARP*S*A-NH_2	>3000	>1000
	Ac-ARP*V*A-NH_2	>3000	>1000
	Ac-ARP*M*A-NH_2	>3000	>1000

Peptides were tested for their capacity to inhibit the interaction of free FGF2 (150 nM) with PTX3 immobilized onto a BIAcore sensor chip and to inhibit the mitogenic activity exerted by FGF2 (0.55 nM) on endothelial GM7373 cells. The experiments were performed with concentrations of peptide ranging between 3 and 3000 μM and between 3 and 1000 μM for the two assays, respectively, and ID_{50} values were calculated from the plotted dose–response curves. Data are representatives of two to three independent experiments in triplicate.

FGF2/FGFR1 interaction without affecting the ability of the growth factor to interact with heparin/HSPGs. This results in the impairment of the formation of a productive HSPG/FGF/FGFR ternary complex, with consequent inhibition of FGFR signalling and FGF2-mediated biological activity.

ARPCA peptide inhibits the angiogenic activity of FGF2 *in vivo*

In a first set of experiments, the capacity of ARPCA to affect FGF2-induced neovascularization *in vivo* was investigated in a chick embryo CAM assay [48]. In this assay, alginate beads adsorbed with FGF2 (8.0 pmoles/embryo) exert a potent angiogenic response when compared with beads adsorbed with vehicle (macroscopic vessels converging towards the implant being equal to 36 ± 4 and 6 ± 3 vessels/embryo, respectively). In keeping with the *in vitro* observations, the angiogenic response elicited by FGF2 was significantly reduced by the addition of 117 nmoles of ARPCA peptide in the FGF2 implants (17 ± 7 vessels/embryo, $P = 0.007$). No effect was instead exerted by control ARPSA (33 ± 5 vessels/embryo) (Fig. 3A).

In a second set of experiments, ARPCA and ARPSA were characterized for their ability to affect the angiogenic response triggered by tumorigenic FGF2-overexpressing mouse aortic endothelial (FGF2-T-MAE) cells in a novel zebrafish embryo/tumour graft model [41, 42]. To this purpose, FGF2-T-MAE cells were resuspended in Matrigel in the absence or in the presence of the peptide under test (300 fmoles/embryo). Then, cells were micro-injected in zebrafish embryos at 48 hrs after fertilization

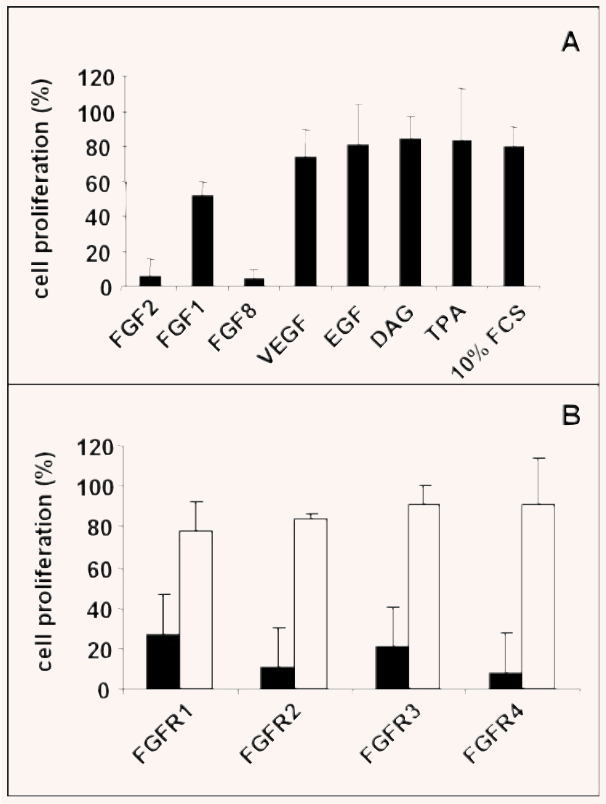

Fig. 1 Effect of Ac-ARPCA-NH_2 on the biological activity of the FGF2/FGFR system. (**A**) GM 7373 cells were treated with FGF2 (0.55 nM), FGF1 (1.66 nM), FGF8b (1.66 nM), VEGF (0.7 nM), EGF (0.6 nM), DAG (15 μM), TPA (8.0 nM) or 10% FCS in the absence or in the presence of Ac-ARPCA-NH_2 (66 μM). (**B**) CHO cells overexpressing FGFR1, FGFR2, FGFR3 or FGFR4 were treated with FGF2 (0.55 nM) in the absence or in the presence of Ac-ARPCA-NH_2 (black bars) or Ac-ARP*S*A-NH_2 (open bars) (both peptides at 300 μM). In both assays, cells were trypsinized and counted 24 hrs after the stimulus. Data (mean ± S.D. of triplicate observations) are expressed as percentage of cell proliferation measured in the absence of the peptide under test.

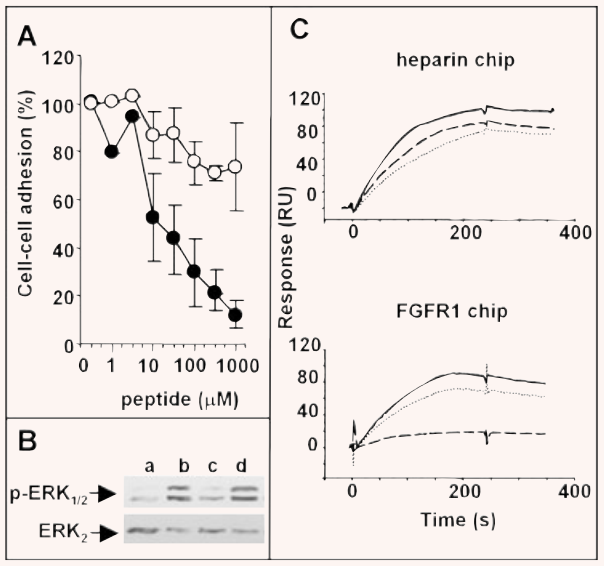

Fig. 2 Effect of Ac-ARPCA-NH_2 on the HSPG/FGF2/FGFR1 complex and FGFR signaling. (**A**) HSPG-deficient, FGFR1-transfected CHO cells were added to wild-type CHO-K1 monolayers in serum-free medium with FGF2 (1.66 nM) in the presence of Ac-ARPCA-NH_2 (●) or Ac-ARP*S*A-NH_2 (○) peptides. After 2 hrs of incubation at 37°C, the cells bound to the monolayer were counted under an inverted microscope. Experiments were performed in triplicate and were repeated twice with similar results. (**B**) GM7373 cells were treated with vehicle (a), 0.17 nM FGF2 (b), or FGF2 *plus* Ac-ARPCA-NH_2 (c) or Ac-ARP*S*A-NH_2 (d) peptides (both at 1.0 mM). After 10 min., cell extracts were analysed by Western blotting using anti-phospho-$ERK_{1/2}$ and anti-ERK_2 antibodies. (**C**) Sensogram overlay showing the binding of FGF2 (150 nM or 50 nM, respectively) to heparin-coated (*upper panel*) or sFGFR1(IIIc)/Fc chimera-coated (*lower panel*) BIAcore sensor chips in the absence (——) or in the presence of Ac-ARPCA-NH_2 (- - -) or Ac-ARP*S*A-NH_2 (·····) peptides (both at 1.0 mM). The response (in RU) was recorded as a function of time.

(1000–2000 cells/embryo) through the perivitelline space between the yolk and the periderm (duct of Cuvier area), close to the developing subintestinal vessels (SIV). As shown in Fig. 3(B), FGF2-T-MAE cell xenografts induced a potent angiogenic response, characterized by newly-formed alkaline phosphatase-positive blood vessels projecting from the SIV plexus, in 87% of injected zebrafish embryos ($n = 19$). This response was significantly reduced to 19% of injected embryos by ARPCA ($n = 16$; $P = 0.002$) but not by ARPSA (72% of positive responses; $n = 14$).

ARPCA/FGF2 interaction mode by NMR spectroscopy

In an attempt to characterize the structural basis and the nature of binding interactions, different NMR experiments were performed on ARPCA peptide alone and in the presence of FGF2. A first set of standard two-dimensional experiments (TOCSY, ROESY, NOESY) were used to assign proton chemical shifts of ARPCA peptide in aqueous solution (Table 3). The analysis of the ROESY experiment, showing only intra-residue and sequential cross-peaks, indicates that ARPCA peptide does not occur in a single, well-defined conformation in aqueous solution. The peptide bond preceding the proline residue is in the *trans* configuration, as deduced from the presence of the Hα Arg2–Hδ1/ Hδ2 Pro3 cross-peaks. The absence of a stable secondary structure for the peptide is confirmed by the measure of $J_{HN\text{-}H\alpha}$ coupling constants, showing average values in the range 5–7 Hz.

In order to map the peptide residues making direct contacts with FGF2, STD NMR methods were applied [46]. STD NMR experiments were performed in the presence of DDT in order to avoid the formation of disulphide bridges between free cysteines. The STD spectrum of ARPCA peptide in the presence of FGF2 proves that methyl protons of Ala1, Ala5 and of the N-terminal

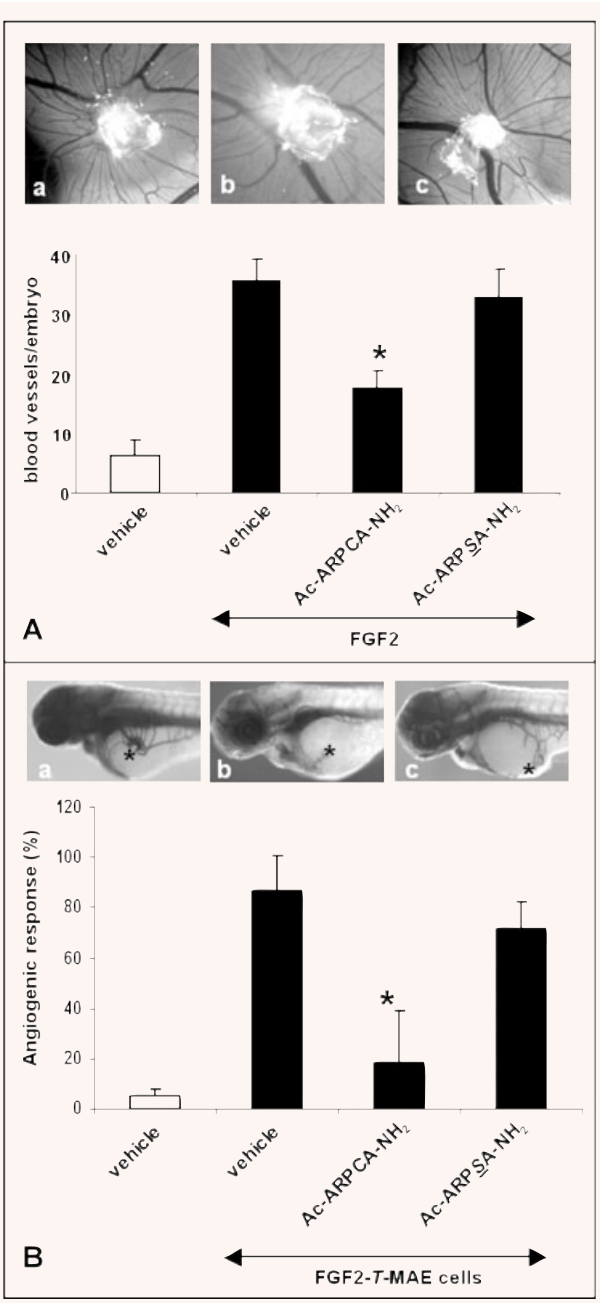

Fig. 3 Anti-angiogenic activity of Ac-ARPCA-NH_2. (**A**) CAMs (10 eggs per group) were implanted at day 11 with alginate beads containing 8 pmoles FGF2 in the absence (a) or in the presence of 117 nmoles of Ac-ARPCA-NH_2 (b) or Ac-ARP<u>S</u>A-NH_2 (c). After 72 hrs, CAMs were photographed *in ovo* (original magnification, ×5) and the blood vessels converging towards the implant were counted (black bars). Alginate beads containing vehicle alone were used as controls (open bar). (**B**) Zebrafish embryos (14–19 embryos per group) were injected with pro-angiogenic tumour FGF2-T-MAE cells resuspended in a Matrigel solution in the absence (a) or in the presence of 300 fmoles/embryo of Ac-ARPCA-NH_2 (b) or Ac-ARP<u>S</u>A-NH_2 (c). After 24 hrs, the percentage of embryos showing a positive angiogenic response, characterized by the growth of alkaline phosphatase-positive SIVs converging *versus* the graft (*), was evaluated (black bars). Embryos injected with Matrigel alone were used as negative controls (open bar). *, $P < 0.05$ or better, Student's t-test.

Table 3 ^{1}H NMR chemical shifts (ppm) of Ac-ARPCA-NH_2 peptide

Amino acid residue	HN	Hα	Hβ	Hγ	Others
N-terminus Ac			2.00		
Ala1	8.41	4.23	1.33		
Arg2	8.55	4.61	1.83	1.71	Hδ 3.20; Hε 7.33
Pro3		4.43	2.29–1.91	2.02	Hδ 3.81–3.64
Cys4	8.66	4.44	2.93		
Ala5	8.63	4.26	1.40		

NMR spectra were recorded at 280 K in 30 mM sodium phosphate buffer, pH 6.8 on a 500 MHz Bruker spectrometer.

blocking acetyl group receive saturation transfer, giving rise to STD NMR signals (Fig. 4A). The hydrophobic patch defined by the three methyl groups is therefore involved in binding to the protein surface. In an attempt to compare the relative contribution of each methyl group to the contact area, a build-up curve of the saturation degree (STD factor, A_{STD}) against the saturation time was performed for each NMR signal (Fig. 4B). It has been previously reported that both the build–up rate and the height of STD factor plateau are strongly affected by T_1 relaxation of the single protons [49]. Indeed at long saturation times higher STD factors are measured for protons with higher T_1 values while at short saturation times, if all sites of the protein are sufficiently saturated, A_{SDT} reflects the average proximity of the ligand protons to the protein surface. Due to the relatively low molecular weight of FGF2, saturation times lower than 1 sec. were not sufficient to saturate the entire protein and to monitor any STD effect. However, from the behaviour of the A_{STD} curves obtained for Ala1 and Ala5 methyl signals, showing comparable T_1 values, a similar contribution to contact area of Ala1 and Ala5 methyls can be inferred. The proximity of the two methyls to FGF2 protein was also evaluated by performing a series of STD titration experiments and calculating the STD factors as a function of ARPCA excess. STD factors obtained for the different chemical groups (Fig. 4C) suggest that the proximity to the protein of the methyl groups of the two Ala residues is comparable. A higher STD amplification factor is observed for the N-terminus acetyl group but the result could be biased by the longer relaxation time T_1 of this group.

In order to investigate the role of the different methyl groups in FGF2 interaction, STD NMR experiments were performed with the ARPCA peptide mutants Ac-*G*RPCA-NH_2, Ac-ARPC*G*-NH_2 and non-acetylated *H*-ARPCA where the single methyl groups were individually removed. The STD spectrum of Ac-*G*RPCA-NH_2 indicates that the peptide is still able to bind FGF2, even though with an affinity slightly lower than ARPCA. The binding mechanism is conserved and the peptide contact area involves the methyl protons of Ala5 and of the N-terminal blocking acetyl group (Fig. 4A and Table 4). On the contrary, the substitution of Ala5 with a Gly residue or the removal of N-terminal acetyl group induce a more dramatic decrease of interaction as deduced from the absence of STD signals for Ac-ARPC*G*-NH_2 and *H*-ARPCA-NH_2, respectively (Fig. 4A). In conclusion, the NMR results point to a hydrophobic interaction of ARPCA with FGF2 mediated by three methyl groups, whose relative position appears to be crucial for FGF2 recognition. However, the three methyls play different roles in the interaction with the protein. Indeed, while the methyls of Ala5 and of the N-terminal blocking acetyl group are essential for FGF2 interaction, the methyl of Ala1 appears to be dispensable, as shown by the retained FGF2-binding ability of the Ac-*G*RPCA-NH_2 mutant.

Discussion

PTX3 comprises a PTX-like C-terminal 203-amino acid domain and an N-terminal 178 amino acid extension with no significant homology with any other protein [26]. Previous observations had shown that PTX3 binds FGF2 with high affinity and selectivity, thus hampering the interaction of the growth factor with its cell surface receptors and inhibiting its activity on target cells [28]. Indeed, PTX3 suppresses the angiogenic activity exerted by FGF2 on endothelial cells [27] and prevents FGF2-dependent smooth muscle cell activation [29], thus representing an endogenous FGF2 inhibitor in different pathophysiological settings and a candidate for the design of novel specific FGF2 antagonists [27].

FGF2 interaction is mediated by the linear amino acid sequence PTX3-(97–110) present in the N-terminal extension on PTX3 [30]. Accordingly, the synthetic peptide PTX3-(97–110) and the longer PTX3-(82–110) peptide prevent FGF2/PTX3 interaction by binding FGF2, thus inhibiting FGF2-dependent endothelial cell proliferation *in vitro* and angiogenesis *in vivo* [30].

Here we have investigated the ability of shorter PTX3-(97–110)-related synthetic peptides to interact with FGF2. The results identify the acetylated pentapeptide ARPCA, corresponding to the amino acid sequence 100–104 in the PTX3 molecule, as the minimal FGF2-binding peptide able to interfere with the biological activity of the growth factor. The peptide prevents the interaction of FGF2 with the full length PTX3 protein and inhibits the mitogenic activity of the growth factor in endothelial cells. This appears to be the consequence of the ability of the peptide to hamper the formation of a productive HSPG/FGF2/FGFR1 ternary complex by inhibiting the binding of FGF2 to its high affinity tyrosine kinase FGFR1 without affecting the interaction with cell surface low affinity HSPGs. This is in keeping with previous observations about the mechanism responsible for the FGF2 antagonist activity of the full length PTX3 protein [28]. The *in vitro* ability of ARPCA peptide to antagonize the activity of FGF2 is reflected *in vivo* by its capacity to suppress the angiogenic activity exerted by the growth factor in the chick embryo CAM assay and that exerted by FGF2-overexpressing tumour cells in a zebrafish embryo/tumour graft assay. Thus, ARPCA peptide is endowed with a significant FGF2-antagonist activity *in vitro* and *in vivo*.

Various amino acid substitutions in the ARPCA sequence, including the removal of the N-terminal blocking acetyl group, cause a dramatic decrease in the FGF2-antagonist activity of the corresponding mutated synthetic pentapeptides (see Table 2), pointing to the relevance of each amino acid residue for ARPCA/FGF2 interaction. On the other hand, STD NMR experiments demonstrate that only the methyl protons of Ala1, Ala5 and of the N-terminal blocking acetyl group receive saturation transfer following FGF2 interaction, indicating that these groups are the main responsible to make a direct contact with FGF2 protein. This suggests that the RPC sequence plays a conformational role in ARPCA/FGF2 interaction and may help to orient the methyl groups of the peptide for optimal interaction with the growth factor. This hypothesis is supported by the lack of FGF2-antagonist activity of the partially scrambled Ac-A*PCR*A-NH_2 mutant and of the scrambled Ac-*PARAC*-NH_2 mutant. In addition, STD NMR experiments show a reduced STD amplification factor for the methyl groups of the Ac-ARP*S*A-NH_2 mutant (data not shown), thus indicating a lower affinity of interaction that results in the lack of FGF2-antagonist activity. Relevant to this point, it is worth noticing that STD NMR experiments were performed under reducing conditions in order to prevent the potential formation of disulphide bridges between Cys4 residues of two ARPCA molecules, leading to the formation of ARPCA dimers, or between Cys4 of ARPCA and free cysteines in the FGF2 protein. Moreover, the observation that amino acid substitution of the cysteine residue or changing its position in the partially scrambled peptide mutants result in a significant inhibition of the FGF2-antagonist activity of the corresponding peptide points to conformational role of Cys4 in ARPCA/FGF2 interaction.

The extracellular portion of FGFRs comprises three Ig-like domains (D1, D2 and D3, with an acidic box between D1 and D2). Their ligand binding and specificity reside in D2, D3 and D2-D3 linker region. X-ray crystallography has shown that the interactions between FGF2 and D3 are of both hydrophobic and polar character whereas the interactions with the D2-D3 linker are mediated mainly *via* hydrogen bonds. At variance, hydrophobic interactions dominate the interface between FGF2 and D2 [50]. Indeed, hydrophobic residues from discontinuous regions in FGF2, including Tyr-24, Phe-31, Tyr-103, Leu-140 and Met-142, form a flat solvent-exposed hydrophobic surface which interacts hydrophobically with Leu-165, Ala-167, Pro-169 and Val-248 of the D2 domain in FGFR1. These residues are well conserved among the four mammalian FGFRs, indicating that this hydrophobic interface represents a highly conserved interaction site for FGF family members [51]. On this basis, it seems possible to suggest that ARPCA peptide may exert its FGF2 antagonist activity by mimicking the

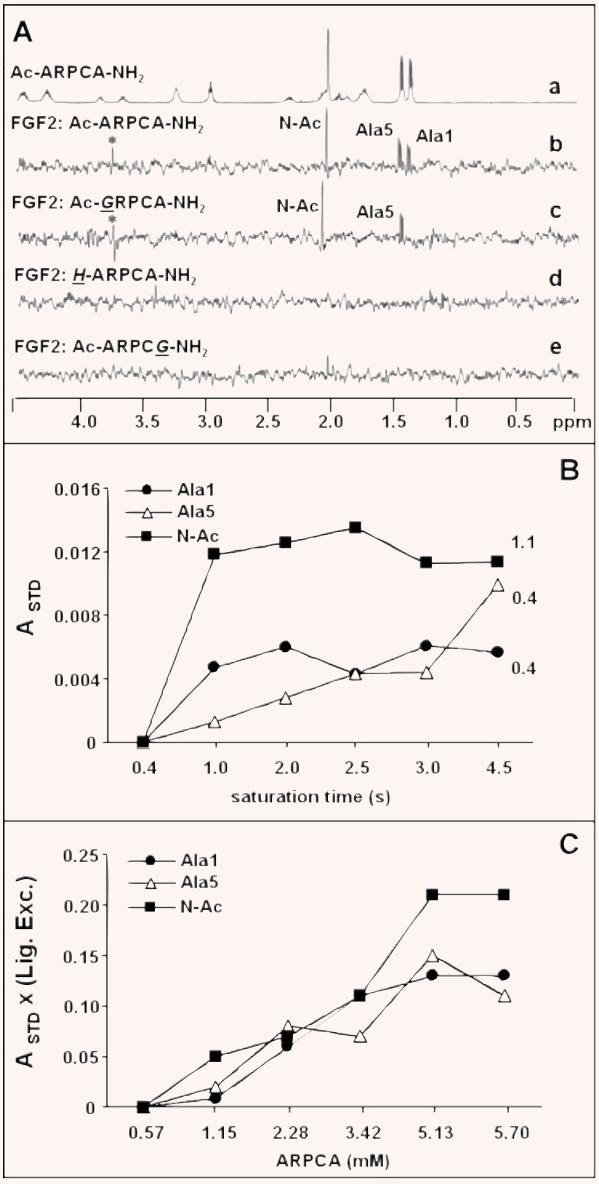

Fig. 4 STD NMR analysis of Ac-ARPCA-NH_2/FGF2 interaction. (**A**) STD spectra of Ac-ARPCA-NH_2 peptide and its mutants acquired at 280 K on a 500 MHz Bruker spectrometer. (a) 1D NMR reference spectrum of 1.9 mM Ac-ARPCA-NH_2 peptide alone; (b)–(e) STD spectra of Ac-ARPCA-NH_2 and the three Ac-*G*RPCA-NH_2, *H*-ARPCA-NH_2 and Ac-ARPC*G*-NH_2 peptides recorded in the presence of 50 μM FGF2 in 30 mM buffer phosphate (95% D_2O, 5% H_2O), 8 mM DTT, 40 mM NaCl, pH 6.8. A saturation time of 3 sec. was used. The assignment of the STD signals is reported. (**B**) Plot of STD factors (A_{STD}) of the Ac-ARPCA-NH_2/FGF2 system *versus* saturation time. A 1:40 FGF2:peptide ratio was used. T_1 relaxation time (sec) of each signal is shown on the right side of the curves. (**C**) A_{STD} × (ligand excess) *versus* different concentrations of Ac-ARPCA-NH_2 peptide.

Table 4 STD NMR analysis of FGF2 interaction with Ac-ARPCA-NH_2 peptide and its mutants: STD amplification factors

	N-terminus Ac	Ala1	Ala5
Ac-ARPCA-NH_2	0.076	0.057	0.077
Ac-*G*RPCA-NH_2	0.032	-	0.066
Ac-ARPC*G*-NH_2	*	*	-
H-ARPCA-NH_2	-	*	*

The effect of the mutation of single methyl groups on the interaction with FGF2 has been characterized by STD experiments. The reported STD amplification factors were calculated as A_{STD} × (ligand excess). An asterisk indicates signals which were not detectable in the STD spectra.

hydrophobic ligand-binding region of D2, thus establishing hydrophobic interactions with the receptor-binding domain of FGF2 and competing with FGFRs for the binding to the growth factor.

Several observations support this hypothesis. (*i*) As stated above, STD NMR experiments have shown that only the methyl protons of Ala1, Ala5 and of the N-terminal blocking acetyl group receive saturation transfer following FGF2 interaction whereas no evidence could be found for hydrophilic contacts between ARPCA peptide and FGF2. Interestingly, hydrophobic interactions with FGF2 have been observed also for the C-terminal fragment of Platelet Factor-4 [52], a well-known anti-angiogenic FGF2 antagonist [53]. (*ii*) ARPCA prevents FGF2/FGFR1 interaction with no effect on the heparin binding capacity of the growth factor. Accordingly, FGFR- and heparin-binding regions represent distinct domains in the FGF2 molecule [14]. (*iii*) ARPCA inhibits FGF2 interactions with all four mammalian FGFRs. (*iv*) ARPCA also inhibits the biological activity of FGF1 and FGF8b without exerting any effect on the activity of different mitogens. (*v*) A model of the proposed interaction was built by conformational analysis (see the 'Computational methods' paragraph in the 'Methods' section and Fig. 5). The conformational analysis performed on ARPCA peptide indicates that the most stable family of conformers show a type-I β-turn between Pro and Cys residues, thus supporting the conformational role of the RPC sequence, and close distances between Ala1 and Ala5 methyls (mean value = 6.6 ± 1.5 Å). The superposition of the global minimum conformation of ARPCA peptide to the β-sheet region 164–170 of the hydrophobic domain D2 of FGFR1 indicated that the peptide could interact with FGF2 by mimicking this highly conserved FGF2-binding region of the receptor. Further experiments are required to confirm this hypothesis.

Interestingly, an anti-angiogenic peptide has been recently identified by screening a phage display heptapeptide library following FGF2 biopanning [25]. At variance with ARPCA, this FGF2-binding peptide shares significant amino acid homology, charge distribution and hydrophobic profile with the Ig-like domain D3 of FGFR1 and FGFR2. Thus, the complexity of FGF2/FGFR interaction is reflected by the possibility to generate various FGF2 antagonists endowed with the capacity to affect this interaction at different levels.

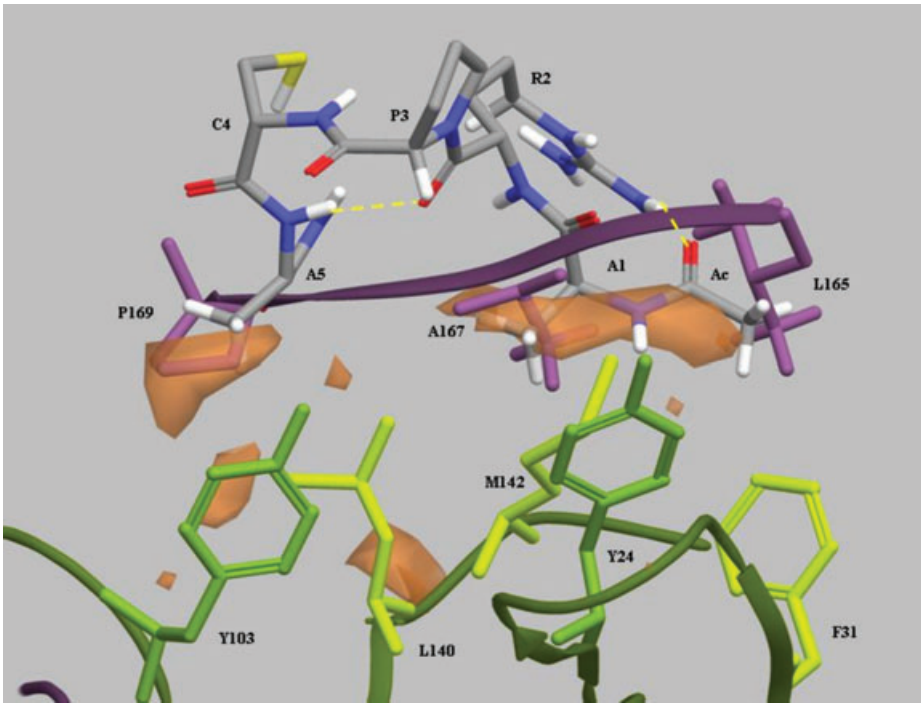

Fig. 5 Hypothesis of interaction between Ac-ARPCA-NH_2 and FGF2. The global minimum conformation of Ac-ARPCA-NH_2 peptide (in atom type in the figure) was superimposed to the crystal structure of FGFR1 (PDB code: 1FQ9) in the β-sheet region 164–170 of the hydrophobic domain D2 of the receptor (FGFR1 residues in purple: Leu165, Ala167 and Pro169). The best superimposition was obtained between the following amino acid pairs of the peptide and receptor, respectively: methyl group of the acetyl cap with Leu165, Ala 1 with Ala167 and Ala5 with Pro169. As shown in the figure, the peptide could mimic the highly conserved β-sheet portion of the receptor interacting with FGF2 (FGF2 residues in green: Tyr24, Phe31, Tyr103, Leu140 and Met142). The hydrophobic characteristics of FGF2 in this region are represented by orange surfaces.

Previous observations had identified the linear amino acid sequence PTX3-(97–110) present in the N-terminal extension on PTX3 as responsible for FGF2/PTX3 interaction. Accordingly, the synthetic peptides PTX3-(97–110) and PTX3-(82–110) are endowed with a significant FGF2-antagonist activity [30]. Here we have demonstrated that this activity is lost when the ARPCA region is mutated within these peptides, thus confirming the importance of the linear ARPCA sequence in FGF2 interaction. In this context, the methyl of the N-terminal blocking group of ARPCA peptide may mimic the hydrophobic side chain of the Leu-99 residue preceding the PTX3-(100–104) ARPCA sequence in the longer PTX3-(97–110) and PTX3-(82–110) peptides and in full length PTX3. Site-directed mutagenesis experiments will be required to assess whether the ARPCA sequence plays a role in the interaction of full length PTX3 protein and/or its N-terminal extension with FGF2.

In conclusion, we have identified the acetylated pentapeptide ARPCA as a short FGF2-binding peptide able to interfere with FGF2/FGFR interaction and to exert a significant FGF2-antagonist activity *in vitro* and *in vivo*. These results will provide the basis for the design of novel PTX3-derived peptidomimetic FGF2 antagonists.

Acknowledgements

We wish to thank Mrs. Michela Corsini for the technical support. This work was supported by grants from Istituto Superiore di Sanità (Oncotechnological Program), Ministero dell'Istruzione, Università e Ricerca (Centro di Eccellenza per l'Innovazione Diagnostica e Terapeutica, Cofin projects), Associazione Italiana per la Ricerca sul Cancro, Fondazione Berlucchi and Fondazione Cariplo (Grant 2008–2264 and NOBEL Project) to M.P.

References

1. **Folkman J.** Angiogenesis in cancer, vascular, rheumatoid and other disease. *Nat Med.* 1995; 1: 27–31.
2. **Carmeliet P, Jain RK.** Angiogenesis in cancer and other diseases. *Nature.* 2000; 407: 249–57.
3. **Keshet E, Ben-Sasson SA.** Anticancer drug targets: approaching angiogenesis. *J Clin Invest.* 1999; 104: 1497–501.
4. **Presta M, Dell'Era P, Mitola S *et al.*** Fibroblast growth factor/fibroblast growth factor receptor system in angiogenesis. *Cytokine Growth Factor Rev.* 2005; 16: 159–78.
5. **Folkman J, Klagsbrun M.** Angiogenic factors. *Science.* 1987; 235: 442–7.
6. **Nugent MA, Iozzo RV.** Fibroblast growth factor-2. *Int J Biochem Cell Biol.* 2000; 32: 115–20.
7. **Gerwins P, Skoldenberg E, Claesson-Welsh L.** Function of fibroblast growth factors and vascular endothelial growth factors and their receptors in angiogenesis. *Crit Rev Oncol Hematol.* 2000; 34: 185–94.
8. **Rusnati M, Presta M.** Fibroblast growth factors/fibroblast growth factor receptors as targets for the development

of anti-angiogenesis strategies. *Curr Pharm Des.* 2007; 13: 2025–44.

9. **Wang Y, Becker D.** Antisense targeting of basic fibroblast growth factor and fibroblast growth factor receptor-1 in human melanomas blocks intratumoral angiogenesis and tumor growth. *Nat Med.* 1997; 3: 887–93.
10. **Rofstad EK, Halsor EF.** Vascular endothelial growth factor, interleukin 8, platelet-derived endothelial cell growth factor, and basic fibroblast growth factor promote angiogenesis and metastasis in human melanoma xenografts. *Cancer Res.* 2000; 60: 4932–8.
11. **Klint P, Claesson-Welsh L.** Signal transduction by fibroblast growth factor receptors. *Front Biosci.* 1999; 4: D165–77.
12. **Schlessinger J, Lax I, Lemmon M.** Regulation of growth factor activation by proteoglycans: what is the role of the low affinity receptors? *Cell.* 1995; 83: 357–60.
13. **Rusnati M, Presta M.** Interaction of angiogenic basic fibroblast growth factor with endothelial cell heparan sulfate proteoglycans. Biological implications in neovascularization. *Int J Clin Lab Res.* 1996; 26: 15–23.
14. **Schlessinger J, Plotnikov AN, Ibrahimi OA *et al.*** Crystal structure of a ternary FGF-FGFR-heparin complex reveals a dual role for heparin in FGFR binding and dimerization. *Mol Cell.* 2000; 6: 743–50.
15. **Cosic I, Drummond AE, Underwood JR *et al.*** In vitro inhibition of the actions of basic FGF by a novel 16 amino acid peptide. *Mol Cell Biochem.* 1994; 130: 1–9.
16. **Ray J, Baird A, Gage FH.** A 10-amino acid sequence of fibroblast growth factor 2 is sufficient for its mitogenic activity on neural progenitor cells. *Proc Natl Acad Sci USA.* 1997; 94: 7047–52.
17. **Williams EJ, Williams G, Howell FV *et al.*** Identification of an N-cadherin motif that can interact with the fibroblast growth factor receptor and is required for axonal growth. *J Biol Chem.* 2001; 276: 43879–86.
18. **Kiselyov VV, Skladchikova G, Hinsby AM *et al.*** Structural basis for a direct interaction between FGFR1 and NCAM and evidence for a regulatory role of ATP. *Structure.* 2003; 11: 691–701.
19. **Neiiendam JL, Kohler LB, Christensen C *et al.*** An NCAM-derived FGF-receptor agonist, the FGL-peptide, induces neurite outgrowth and neuronal survival in primary rat neurons. *J Neurochem.* 2004; 91: 920–35.
20. **Anderson AA, Kendal CE, Garcia-Maya M *et al.*** A peptide from the first fibronectin domain of NCAM acts as an inverse agonist and stimulates FGF receptor activation, neurite outgrowth and survival. *J Neurochem.* 2005; 95: 570–83.
21. **Berezin V, Bock E.** NCAM mimetic peptides: an update. *Adv Exp Med Biol.* 2010; 663: 337–53.
22. **Hansen SM, Li S, Bock E *et al.*** Synthetic NCAM-derived ligands of the fibroblast growth factor receptor. *Adv Exp Med Biol.* 2010; 663: 355–72.
23. **Hagedorn M, Zilberberg L, Lozano RM *et al.*** A short peptide domain of platelet factor 4 blocks angiogenic key events induced by FGF-2. *FASEB J.* 2001; 15: 550–2.
24. **Facchiano A, Russo K, Facchiano AM *et al.*** Identification of a novel domain of fibroblast growth factor 2 controlling its angiogenic properties. *J Biol Chem.* 2003; 278: 8751–60.
25. **Wu X, Yan Q, Huang Y *et al.*** Isolation of a novel basic FGF-binding peptide with potent antiangiogenetic activity. *J Cell Mol Med.* 2010; 14: 351–6.
26. **Garlanda C, Bottazzi B, Bastone A *et al.*** Pentraxins at the crossroads between innate immunity, inflammation, matrix deposition, and female fertility. *Annu Rev Immunol.* 2005; 23: 337–66.
27. **Presta M, Camozzi M, Salvatori G *et al.*** Role of the soluble pattern recognition receptor PTX3 in vascular biology. *J Cell Mol Med.* 2007; 11: 723–38.
28. **Rusnati M, Camozzi M, Moroni E *et al.*** Selective recognition of fibroblast growth factor-2 by the long pentraxin PTX3 inhibits angiogenesis. *Blood.* 2004; 104: 92–9.
29. **Camozzi M, Zacchigna S, Rusnati M *et al.*** Pentraxin 3 inhibits fibroblast growth factor 2-dependent activation of smooth muscle cells in vitro and neointima formation in vivo. *Arterioscler Thromb Vasc Biol.* 2005; 25: 1837–42.
30. **Camozzi M, Rusnati M, Bugatti A *et al.*** Identification of an antiangiogenic FGF2-binding site in the N terminus of the soluble pattern recognition receptor PTX3. *J Biol Chem.* 2006; 281: 22605–13.
31. **Isacchi A, Statuto M, Chiesa R *et al.*** A six-amino acid deletion in basic fibroblast growth factor dissociates its mitogenic activity from its plasminogen activator-inducing capacity. *Proc Natl Acad Sci USA.* 1991; 88: 2628–32.
32. **Rivieccio V, Esposito A, Bellofiore P *et al.*** High-level expression and efficient purification of recombinant human long pentraxin PTX3 in Chinese hamster ovary cells. *Protein Expr Purif.* 2007; 51: 49–58.
33. **Esko JD.** Genetic analysis of proteoglycan structure, function and metabolism. *Curr Opin Cell Biol.* 1991; 3: 805–16.
34. **Liekens S, Leali D, Neyts J *et al.*** Modulation of fibroblast growth factor-2 receptor binding, signaling, and mitogenic activity by heparin-mimicking polysulfonated compounds. *Mol Pharmacol.* 1999; 56: 204–13.
35. **Rusnati M, Dell'Era P, Urbinati C *et al.*** A distinct basic fibroblast growth factor (FGF-2)/FGF receptor interaction distinguishes urokinase-type plasminogen activator induction from mitogenicity in endothelial cells. *Mol Biol Cell.* 1996; 7: 369–81.
36. **Ribatti D, Gualandris A, Belleri M *et al.*** Alterations of blood vessel development by endothelial cells overexpressing fibroblast growth factor-2. *J Pathol.* 1999; 189: 590–9.
37. **Presta M, Maier JA, Rusnati M *et al.*** Basic fibroblast growth factor: production, mitogenic response, and post-receptor signal transduction in cultured normal and transformed fetal bovine aortic endothelial cells. *J Cell Physiol.* 1989; 141: 517–26.
38. **Leali D, Belleri M, Urbinati C *et al.*** Fibroblast growth factor-2 antagonist activity and angiostatic capacity of sulfated Escherichia coli K5 polysaccharide derivatives. *J Biol Chem.* 2001; 276: 37900–8.
39. **Bugatti A, Urbinati C, Ravelli C *et al.*** Heparin-mimicking sulfonic acid polymers as multitarget inhibitors of HIV-1 Tat and gp120 proteins. *Antimicrob Agents Chemother.* 2007; 51: 2337–45.
40. **Knoll A, Schmidt S, Chapman M *et al.*** A comparison of two controlled-release delivery systems for the delivery of amiloride to control angiogenesis. *Microvasc Res.* 1999; 58: 1–9.
41. **Nicoli S, Presta M.** The zebrafish/tumor xenograft angiogenesis assay. *Nat Protoc.* 2007; 2: 2918–23.
42. **Nicoli S, Ribatti D, Cotelli F *et al.*** Mammalian tumor xenografts induce neovascularization in zebrafish embryos. *Cancer Res.* 2007; 67: 2927–31.
43. **Serbedzija GN, Flynn E, Willett CE.** Zebrafish angiogenesis: a new model for drug screening. *Angiogenesis.* 1999; 3: 353–9.
44. **Bax D, Davis GD.** MLEV-17-based two-dimensional homonuclear magnetization transfer spectroscopy. *J Magn Reson.* 1985; 65: 355–60.
45. **Hwang TL, Shaka AJ.** Water suppression that works. Excitation sculpting using arbitrary wave-forms and pulsed-field gradients. *J Magn Reson Series A.* 1995; 112: 275–9.

46. **Mayer M, Meyer B.** Group epitope mapping by saturation transfer difference NMR to identify segments of a ligand in direct contact with a protein receptor. *J Am Chem Soc.* 2001; 123: 6108–17.
47. **Ornitz DM, Xu J, Colvin JS *et al.*** Receptor specificity of the fibroblast growth factor family. *J Biol Chem.* 1996; 271: 15292–7.
48. **Ribatti D, Nico B, Vacca A *et al.*** The gelatin sponge-chorioallantoic membrane assay. *Nat Protoc.* 2006; 1: 85–91.
49. **Yan J, Kline AD, Mo H *et al.*** The effect of relaxation on the epitope mapping by saturation transfer difference NMR. *J Magn Reson.* 2003; 163: 270–6.
50. **Mohammadi M, Olsen SK, Ibrahimi OA.** Structural basis for fibroblast growth factor receptor activation. *Cytokine Growth Factor Rev.* 2005; 16: 107–37.
51. **Plotnikov AN, Hubbard SR, Schlessinger J *et al.*** Crystal structures of two FGF-FGFR complexes reveal the determinants of ligand-receptor specificity. *Cell.* 2000; 101: 413–24.
52. **Ragona L, Tomaselli S, Quemener C *et al.*** New insights into the molecular interaction of the C-terminal sequence of CXCL4 with fibroblast growth factor-2. *Biochem Biophys Res Commun.* 2009; 382: 26–9.
53. **Bikfalvi A.** Platelet factor 4: an inhibitor of angiogenesis. *Semin Thromb Hemost.* 2004; 30: 379–85.